ISSN 1560-0904, Polymer Science, Series B, 2021, Vol. 63, No. 4, pp. 367–384. © Pleiades Publishing, Ltd., 2021.
Russian Text © The Author(s), 2021, published in Vysokomolekulyarnye Soedineniya, Seriya B, 2021, Vol. 63, No. 4, pp. 231–250.

DEGRADATION OF POLYMERS

Features of Thermo-Oxidative Degradation of Epoxy Oligomer-Based Compositions with Thermoplastic Fillers

L. S. Shibryaeva[a,*], I. Yu. Gorbunova[b], M. L. Kerber[b], and P. A. Povernov[a]

[a] *Emanuel Institute of Biochemical Physics, Russian Academy of Sciences, Moscow, 119334 Russia*
[b] *Mendeleev University of Chemical Technology, Moscow, 125047 Russia*
**e-mail: lyudmila.shibryaeva@yandex.ru*

Received December 17, 2020; revised April 1, 2021; accepted April 14, 2021

Abstract—The effect of fillers, polysulfone and polyetherimide, on the mechanism and kinetics of the thermo-oxidative degradation of a composition based on an epoxy oligomer cured with 4,4'-diaminodiphenyl sulfone which proceeds under heating in the nonisothermal regime is studied. A relationship is revealed between the structure of the composition and the mechanism and kinetic parameters of the process, on one hand, and the chemical nature of the filler, on the other hand. Mechanistic and kinetic features of the nonisothermal degradation of the epoxyamine composition are ascertained by the thermoanalytical method using differential scanning calorimetry. The kinetic parameters of the process are assessed by an analysis of thermokinetic curves in terms of thermokinetic models and the examination of oxidation products. Depending on the filler nature and composition structure, reactions involving bonds of interjunction chains and junctions of the network of the epoxy polymer as well as radical reactions of the active centers of the filler occur in the polymer during thermal oxidation. An increase in the network density and the localization of the filler determine the contribution of the diffusion factor, decrease the rate of thermo-oxidative degradation of interjunction chains, and increase the rate of breakdown of network junctions.

DOI: 10.1134/S1560090421040096

INTRODUCTION

Materials based on epoxy compositions are in common use in diverse industries. A demanding issue arising in the production and processing of these compositions is to ensure their stability at elevated temperatures in an air medium. At the same time, the service conditions of epoxy materials require improvement in their thermal stability and resistance against thermal and thermo-oxidative degradation. These tasks can be solved through modification of epoxy compositions by introducing various fillers [1–15]. For example, nanofillers (silver, titania, ethoxysilane, clay, and montmorillonite species [3–8]) and compounds such as phosphazenes, carboxyl-containing rubbers, aromatic polyethers, and thermoplastics are in wide use as fillers [9–17]. Modification affects the cure mechanism of the epoxy oligomer and thus changes the physicochemical properties of the compositions. There are different and sometimes contradictory data on the effect of modifiers on the thermal stability of epoxy compositions [18–20]. This is associated with the fact that the thermal and thermo-oxidative stability of polymers depends on a number of factors.

The study of the thermal oxidation of polymers based on epoxy resins demonstrated the leading role of such factors as supramolecular and molecular structure of a binder. Experiments on the thermo-oxidative degradation of an unfilled polymer based on epoxy resin ED-20 cured with 4,4'-diaminodiphenyl sulfone in different cure modes showed that the kinetics and mechanism of the process are affected by the network density and segmental mobility; these parameters determine the ratio between the rates of thermal oxidation, degradation of interjunction chains, and breakdown of network junctions [20].

The modification of epoxy compositions creates prerequisites for a considerable change in the regularities of oxidation and degradation of the material owing to participation of the modifier in the processes of both cure of the composition and its oxidation. The laws of the thermo-oxidative degradation of modified epoxy compositions filled with various classes of compounds differ according to the nature of the filler [4–6, 16, 17, 20–25].

For example, the data available for amine-cured epoxy-silica composites based on the epoxy resin EPONEX-1510 and the products of tetraethoxysilane hydrolysis at a silica filler concentration of 12.5 wt % or above show that filled epoxy polymers possess higher thermal stability and resistance to oxidative processes than unfilled polymers [6, 23]. Note that an organic filler inhibits the oxidation of composites: the maximum rate of oxygen absorption decreases and the onset temperature of the main stage of thermo-oxida-

tive degradation considerably shifts to higher temperatures. The rate of oxygen absorption by the samples is almost independent of the content of silica in composites [6].

Research into the effect of titanium oxide filler on the kinetics of thermo-oxidative degradation of the polymer matrix in glassy epoxy-titanium composites indicated that the high-temperature stability of composite materials and their oxidation resistance depend on the concentration of the filler. Systems containing from 0.5 to 1.5 wt % TiO_2 are more stable to thermal oxidation than the initial epoxy polymer. Moreover, the maximum rate of oxygen absorption by the composites is 4–13 times lower than the rate of oxidation of the initial polymer [4, 5].

As exemplified by composites filled with oligoesters [17] the thermo-oxidative stability of the system primarily depends on the chemical nature of the modifier. Introduction of the filler may cause either a marked increase or decrease in its oxidation rate [17, 23]. An increase in the rate of the process is associated with a reduction in the concentration of functional epoxy groups involved in the formation of network structures owing to dilution of the epoxy system with the filler [17]. The filler may exert an inhibiting effect or create diffusion limitations to the delivery of oxygen to the matrix [17, 22, 23]; as a result, the rate of thermal oxidation of the composition decreases.

In accordance with the published data, the kinetics and mechanism of thermal and thermo-oxidative degradation of filled and modified samples depend, first, on structural factors and, second, on the type of chemical reactions between functional groups in macromolecules of the epoxy binder and modifying components.

It is important to mention that the mechanism of degradation of a filled or plasticized epoxy composition is controlled by diffusion processes; as a consequence, it may include several types of reactions occurring according to different schemes. Reaction schemes may change during the thermo-oxidative degradation of the epoxy composition owing to the accumulation of oxidation products [22].

In tackling the problem of enhancing thermal and thermo-oxidative stability of epoxy materials, gaining insight into the role of each of the mentioned factors influencing the thermo-oxidative degradation of epoxy compositions in accordance with the modifier nature is an urgent task.

The goal of this work is to unveil kinetic and mechanistic features of the thermo-oxidative degradation of the epoxyamine polymer modified with thermoplastic fillers of various nature in relation to the structure of the network formed during preliminary cure of the polymer.

EXPERIMENTAL

An object of research was the epoxy oligomer ED-20 (commercial resin) with $M_n = 390$ cured with 4,4'-diaminodiphenyl sulfone (**DADPS**) at a ratio of 70 : 30 (phr). This ratio makes it possible to reach the maximum glass transition temperature (200°C). Modifiers introduced in the epoxy composition were aromatic polyethers (5 phr): polysulfone (**PSF**) Ultrason S-2010 (BASF) with $M_w = 3.5 \times 10^4$ and the glass transition temperature $T_g = 191$°C and polyetherimide Ultem-1010 (General Electric) with $M_w = 3.0 \times 10^5$ and $T_g = 216$°C.

Blends of the epoxy oligomer with polyethers were obtained by dissolving polymer granules in the oligomer at 120 (polysulfone) or 150°C (polyetherimide) under mechanical mixing.

The rheological behavior of ED-20 blend compositions with polyethers was investigated on a Physica MCR-301 rotational rheometer (Anton Paar) in the controlled stress mode using the plate-plate operating unit. The shear stress was varied from 0.01 to 100 Pa, and the temperature was varied in the range from 20 to 200°C. Dynamic tests were carried out in the region of linear viscoelasticity of the samples in the angular frequency range of 0.0628–628 s^{-1}.

The systems were cured in three modes: the stepwise mode, in which cure was carried out at 160–180–200°C for 2–4–2 h, respectively; and the isothermal mode at two temperatures 180 and 200°C for 12 h.

The degree of cure was estimated by DSC from the amount of released heat measured by a Netzsch DSC-204 F1 Phoenix calorimeter as well as by dynamic mechanical analysis (**DMA**) on a MK-3 torsion pendulum in the regime of freely decaying oscillations; the loss tangent tan δ and the shear storage modulus G' were determined [13].

The glass transition temperature was estimated by DSC and the thermomechanical method using a Höppler consistometer.

The degradation processes of filled epoxy polymers were studied by DSC on a Netzsch Polyma-214 microcalorimeter (Germany). Heating and cooling of the samples were carried out in the temperature range of 30–500°C at a scan rate of 4°C/min. Weighed portions of the samples were (5.0 ± 0.1) and (10.0 ± 0.1) mg. Experiments were performed in an air stream at a flow velocity of ~15 mL/min. The thermal effects accompanying the thermal and thermo-oxidative degradations of the material were measured. The temperature scale and the enthalpy of melting were calibrated with respect to the indium standard sample (the melting temperature $T_m = 156.6$°C, and the specific heat of melting $\Delta H = 28.44$ J/g). The temperature determination was accurate to within ±0.5°C.

The obtained thermophysical curves of thermo-oxidative degradation were analyzed by the thermokinetic method using various models describing tem-

perature dependences for the rate of chemical processes and the conversion of compounds in them.

The mean square deviations of the experimental values of the area under thermodegradation peaks for different samples were within 10%.

The IR spectra of the cured film samples were measured on a Nicolet-380 spectrometer in the wavenumber range from 400 to 4000 cm^{-1}. Transparent films with a thickness of 60–100 μm were prepared for the IR analysis. The content of functional groups was calculated from the ratio between the optical density of functional groups and the reference peak characterizing the thickness of the sample. Errors in the determination of the parameters were ±10%.

RESULTS AND DISCUSSION

To learn the kinetic and mechanistic features of the thermal oxidation and thermo-oxidative degradation of the epoxyamine composition filled with thermoplastics, modifiers compatible with the oligomer were chosen and samples precured in different modes were prepared. Samples filled with polysulfone soluble in the oligomer and with polyetherimide incompatible with the epoxy oligomer, accordingly, forming homogeneous, single-phase, and heterophase systems were studied [14]. The cure of the epoxy oligomer with DADPS in the presence of soluble PSF and insoluble polyetherimide was examined in [15, 17]. It was shown that introduction of the thermoplastic modifier in the composition changes the structure of the network and its density depending the type of phase structure formed in the matrix when the epoxy oligomer is cured in the presence of fillers.

When choosing the objects of research, the authors of [15, 17] assumed that the effect of modifiers, polyetherimide and PSF, on the reactivity of an epoxyamine polymer in the process of thermo-oxidative degradation and its mechanism and kinetics will be defined by both the heterophase state of the system and the structure of the network of the epoxy matrix and the chemical nature of the components.

For a more detailed study of the role of network structure composition, we chose samples precured at 180 and 200°C for 12 h as well as in the stepwise mode at 160–180–200°C treated for 2–4–2 h, respectively.

In accordance with [13, 17, 20], the glass transition temperature and the impact strength can be used as indicators of the structural parameters of initial and filled epoxyamine compositions. These parameters for the tested systems are summarized in Table 1. For example, for the samples of the initial epoxyamine polymer, T_g increases and the impact strength remains unchanged with an increase in the cure temperature. For the modified samples, T_g grows compared with the unmodified samples regardless of the cure temperature. For the sample filled with polyetherimide, T_g is higher than that of the sample filled with PSF; this fact is evidence for a lower mobility of chains. The impact strength for the system containing PSF decreases with increasing cure temperature, while for the samples containing polyetherimide the impact strength changes in a complex manner. These results testify that the structures of networks of initial and modified epoxyamine compositions are different, in agreement with the data described in [13, 14, 24]. The nature of the dependence of T_g and the impact strength on the cure mode for the modified samples may be explained by the different structure of amorphous zones between network junctions and the nature of filler localization in these zones. It should be noted that, for the sample with polyetherimide, the filler is distributed in the form of phase particles inserted into the network of the epoxy polymer, while for the sample with PSF the filler is distributed in the form of macromolecules [7].

The process of thermal oxidation of epoxy compositions in an air or oxygen medium can be described by the kinetic scheme of the chain process with the degenerate branching of kinetic chains [25–27].

Initiation of kinetic oxidation chains

$$R_{1,2,\ldots n}H + O_2 \rightarrow R^{\bullet}_{1,2,\ldots n}(k_{0\,1,2,\ldots n}) + HO^{\bullet}_2$$

$$R_{1,2,\ldots n}H \rightarrow R^{\bullet}_{1,2,\ldots n}(k'_{0\,1,2,\ldots n})$$

Propagation of kinetic chains

$$R^{\bullet}_{1,2,\ldots n} + O_2 \rightarrow R_{1,2,\ldots n}O^{\bullet}_2(k_{1\,1,2,\ldots n})$$

$$R_{1,2,\ldots n}O^{\bullet}_2 + R_{1,2,\ldots n}H \rightarrow R_{1,2,\ldots n}OOH + RO^{\bullet}_{1,2,\ldots n}(k_{2\,1,2,\ldots n})$$

Branching of kinetic chains

$$\delta R_{1,2,\ldots n}OOH \rightarrow \sigma R^{\bullet}_{1,2,\ldots n} + H_2O\,(k_{3\,1,2,\ldots n})$$

Termination of kinetic chains

$$R^{\bullet}_{1,2,\ldots n} + R^{\bullet}_{1,2,\ldots n} \rightarrow \text{inactive products}\ (k_{4\,1,2,\ldots n})$$

$$R_{1,2,\ldots n}O^{\bullet}_2 + R_{1,2,\ldots n}O^{\bullet}_2 \rightarrow \text{inactive products}\ (k_{6\,1,2,\ldots n})$$

Here $R_{1,2,\ldots n}OOH$, $R^{\bullet}_{1,2,\ldots n}$, $R_{1,2,\ldots n}O^{\bullet}_2$, and $R_{1,2,\ldots n}H$ are hydroperoxide, alkyl radical, peroxide radical, and polymer bond R–H, respectively; indices 1, 2, ...*n* at reaction scheme elements refer to each component of the epoxy composition, modifier molecules, epoxy matrix chains appearing in interjunction chains, and network junctions participating in the oxidation reaction; they depict reactions for each component with its index; O_2 is an oxygen molecule; $k_{1\,1,2,\ldots n}$, $k_{2\,1,2,\ldots n}$, $k_{3\,1,2,\ldots n}$, $k_{4\,1,2,\ldots n}$, $k_{5\,1,2,\ldots n}$, and $k_{6\,1,2,\ldots n}$ are the rate constants of elementary stages of the oxidation process; δ is the yield of hydroperoxide per mole of absorbed oxygen, $\delta < 1$; and σ is the probability of the degenerate branching of kinetic chains, $\sigma < 2$.

Table 1. Glass transition temperature, impact strength, and parameters of the thermo-oxidative process for the initial compositions and polyetherimide- and PSF-filled compositions based on the epoxy resin ED-20 and DADPS

Cure mode		Physicochemical parameters		Parameters of thermo-oxidative degradation		
T, °C	time, h	T_g, °C	impact strength, kJ/m^2	T_{ini}, °C	$T_{=0.1}-T_{ini}$*, °C (time, s)	$(dH(t)/dt)^{0.5} = f(t)$**, arb. units/s (ΔT, °C)
ED-20 + DADPS						
160–180–200	2–4–2	160	6	385 ± 10	385–404 (285)	6.3×10^{-4} (384–450)
180	12	165	6	355 ± 10	355–377 (330)	6.4×10^{-4} (362–440)
200	12	170	6	393 ± 10	393–409 (240)	8.5×10^{-4} (400–418)
						5.5×10^{-4} (418–450)
ED-20 + DADPS + polyetherimide						
160–180–200	2–4–2	180	12	344 ± 10	344–368 (360)	6.0×10^{-4} (340–424)
180	12	180	5	353 ± 10	353–386 (495)	5.6×10^{-4} (364–436)
200	12	180	12	398 ± 10	398–414 (240)	5.4×10^{-4} (410–425)
						4.1×10^{-4} (426–438)
ED-20 + DADPS + PSF						
160–180–200	2–4–2	175	15	283 ± 10	283–298 (225)	8.8×10^{-4} (280–336)
180	12	175	9	320 ± 10	320–338 (270)	11.1×10^{-4} (320–368)
200	12	172	8	333 ± 10	333–343 (150)	9.1×10^{-4} (337–373)

*Characteristic of the induction period: $T_{=0.1}$ is temperature corresponding to the polymer conversion during degradation $\alpha = 10\%$, and $T_{=0.1}-T_{ini}$ is the temperature and time interval between the initial temperature and $T_{=0.1}$ corresponding to the induction period of thermo-oxidative degradation.

**Slope of the linear anamorphosis of the kinetic curve in coordinates $(dH(t)/dt)^{0.5} = f(t)$ on the time axis (time corresponding to the T_{ini} of the DSC thermogram was taken as the zero time $t = 0$); this parameter is assigned to the mentioned temperature interval corresponding to the anamorphosis (ΔT, °C).

The process of thermo-oxidative degradation proceeds at the stage of propagation and termination of kinetic chains. The stage of propagation includes reactions

$$RO_2^{\bullet} + RH \rightarrow [ROOH + R^{\bullet}]$$

$$\rightarrow \delta ROOH + R^{\bullet} + (1 - d)\ (>C=O, -OH).$$

In the oxidation of solid polymers at the stage of propagation of kinetic chains, the reaction of group ROOH with radical R$^{\bullet}$ occurs to give rise to carbonyl >C=O and hydroxyl groups simultaneously with the breakage of C–C bonds of macromolecules.

At the stage of termination, hydroxyl and carbonyl groups are formed:

$$RO_2^{\bullet} + RO_2^{\bullet} \rightarrow ROH + R''COR + O_2.$$

The presence of several active components in the epoxy composition, as well as the difference in active centers in the epoxy matrix, complicates this scheme. Within each stage, cross reactions may be realized, for example, at the stage of propagation of kinetic oxidation chains:

$$R_1O_2^{\bullet} + R_2H \rightarrow R_2OOH + R_1^{\bullet}\ (k_{21}).$$

Cross reactions may lead either to deceleration of the process or to its acceleration depending on the nature and activity of components, free valence carriers.

The presence of nonvolatile products of chain oxidation, carbonyl-containing and hydroxyl-containing fragments, was confirmed by IR spectroscopy.

Owing to the complex scheme of the process, the kinetic aspect of degradation of epoxy compositions in the air medium under the dynamic heating of the sample is considered using the thermokinetic method. This method is based on the assumption that the temperature of the sample is uniform and the degradation can be described by the equation of reaction (in Arrhenius coordinates):

$$d[RH]/dt = (1 - [RH])^n A \exp(E_a/RT),$$

where [RH] is the concentration of active bonds, E_a is the activation energy, A is the pre-exponential factor, and n is the reaction order.

In this work, the rate of the process is estimated from the time dependence of the amount of heat released during thermo-oxidative degradation. Kinetic calculations are carried out using the results of DSC measurements. The rate of reaction is propor-

tional to the rate of a change in the heat flow [28–30]; i.e., the expression

$$d\alpha/dt = 1/H_{tot}(dH(t)/dt), \quad (1)$$

is valid, where α is the conversion of the polymer equal to dH_t/H_{tot}, which corresponds to ~$[RH]_t/[RH]_{tot}$; $d\alpha/dt$ is the rate of a change in conversion; H_{tot} is the total enthalpy of the reaction; and $dH(t)/dt$ is the rate of change in the heat flow.

It is substantial that the obtained DSC curves can be used for both calculating the kinetic parameters and approximating by the kinetic model. The same DSC curve can be used to determine the values of E_a, A, and n.

In this work, DSC thermograms were measured in the nonisothermal regime during heating of the samples at a constant rate β equal to 4°C/min in the temperature range of 200–500°C. The thermograms of all the tested samples show exothermic peaks of thermo-oxidative degradation (Fig. 1). It is seen that the DSC data are in agreement with TGA and DTA studies. This makes it possible to use thermokinetic methods of the former technique by analogy with the latter techniques. Using graphical differentiation and integration of thermo-oxidative degradation exotherms over time and temperature, kinetic curves characterizing the rate of change in the specific heat release during thermal oxidation were obtained for all the tested samples, as well as temperature dependences corresponding to these curves. Figure 2 presents the temperature dependences of change in the rate of heat release $dH(t)/dt = f(T)$ during the thermo-oxidative degradation of epoxyamine compositions ED-20 + DADPS, initial and filled with polyetherimide and PSF, cured in different modes. It is seen that the shape of the kinetic curves is typical of autocatalytic radical-chain oxidation with the degenerate branching of kinetic chains, which matches the above-described scheme; this is consistent with the data reported for the epoxyamine polymer [17, 20]. Hence, the kinetic curve describes the initial stage with the slowed down rate (the induction period τ_{ind}) and the self-accelerated region of thermo-oxidative degradation and characterizes the kinetic parameters of oxidation. The time corresponding to a difference between the initial temperature of exothermic peaks T_{ini} and the temperature corresponding to a polymer conversion of up to 10% ($T_{\alpha=0,1}T_{ini}$) may be taken as the induction period. The slopes of linear anamorphoses of the curves $dH/dt = f(T)$ represented in the coordinates of parabola $(dH(t)/dt)^{0.5} = f(t)$ and by the time interval axis may be regarded as a factor characterizing the self-acceleration parameter.

The above parameters of activity in thermo-oxidative degradation obtained for the tested samples are correlated with their structural parameters in Table 1. Figure 2 primarily demonstrates the most evident difference in the activities of unfilled, incompatible, and compatible systems (curves *1–3*, respectively). Given this, the differences between curves *1* and *2* are less distinct compared with the compatible system containing PSF (curve *3*). For all samples, the differences at the initial stage of the process depend on the precure conditions of the compositions. For the compatible system with PSF, the onset temperature of degradation of the epoxyamine composition decreases by 100°C for the sample cured in the stepwise mode (Table 2) and by 40 and 60°C for the samples cured at

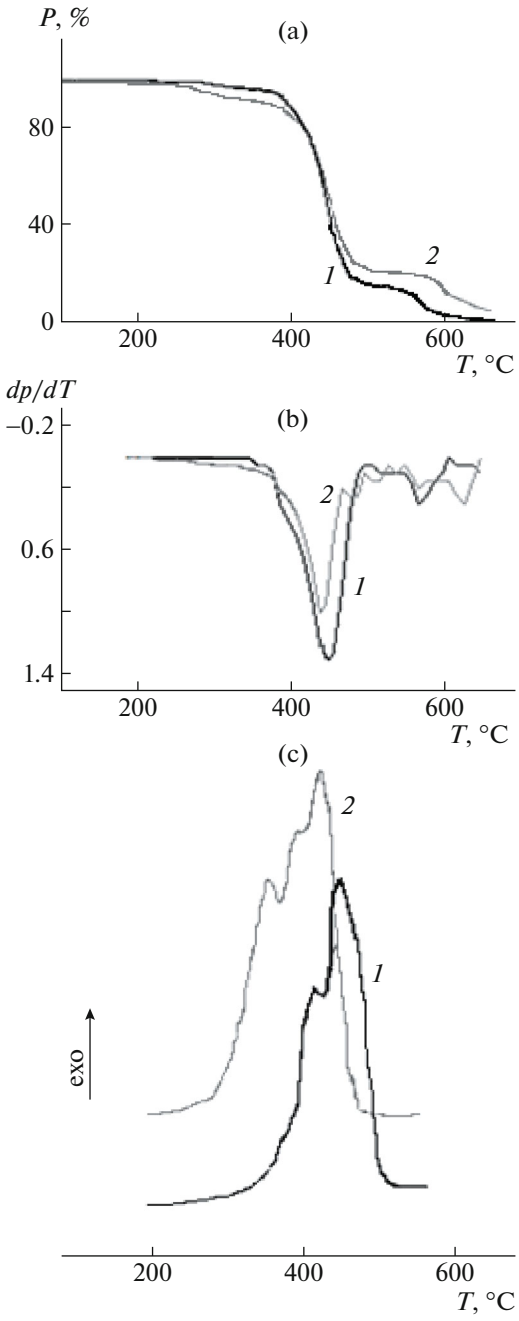

Fig. 1. (a) TGA, (b) DTA, and (c) DSC curves for (*1*) ED-20 + DADPS and (*2*) ED-20 + DADPS + PSF precured at 200°C for 12 h.

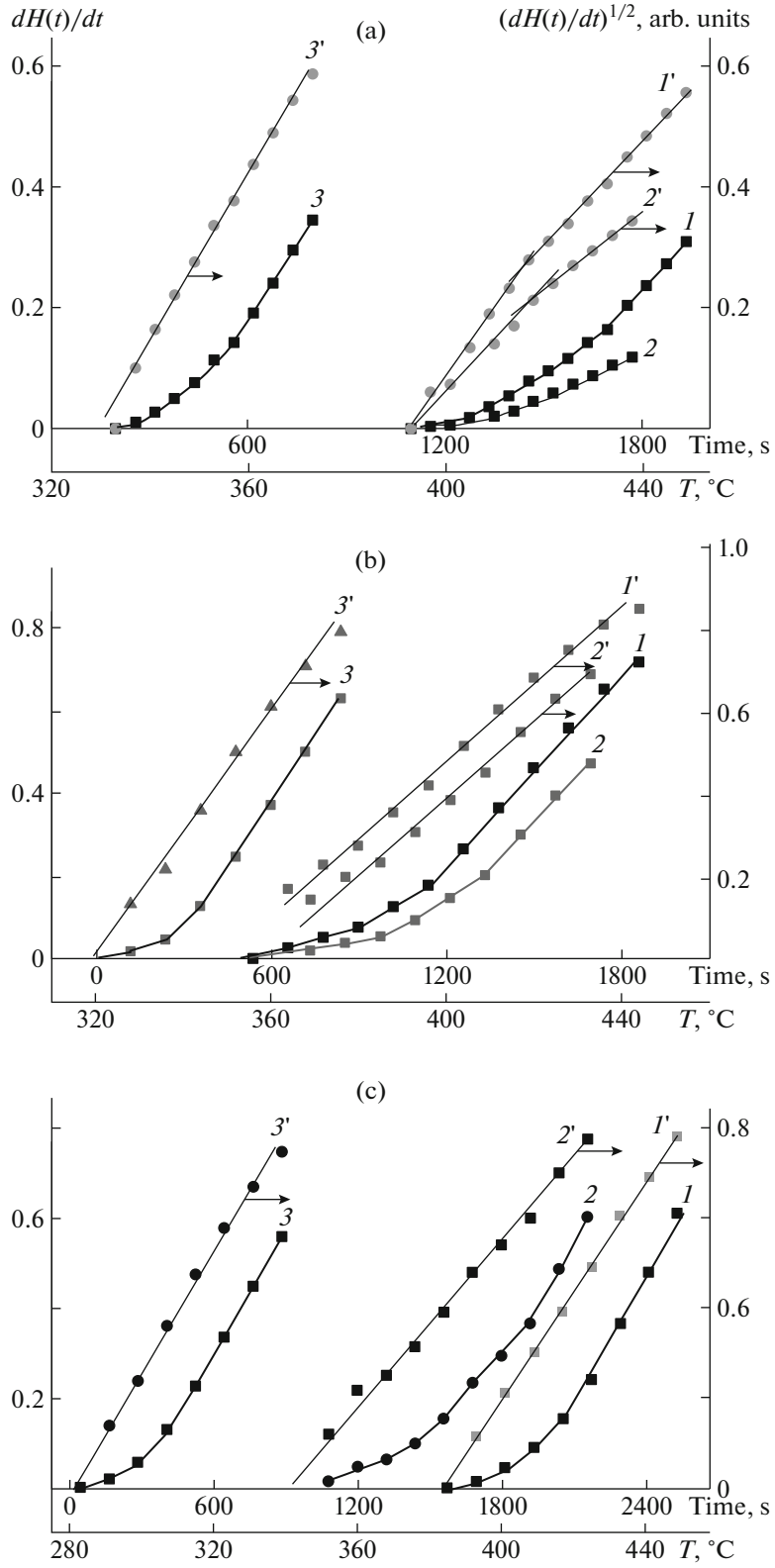

Fig. 2. (*1*–*3*) Thermokinetic curves of change in the heat of thermo-oxidative degradation during the process expressed in coordinates $dH(t)/dt = f(t)$ and (*1'*–*3'*) their linear anamorphoses in the coordinates of parabola $(dH(t)/dt)^{0.5} = f(t)$ for the samples of (*1*, *1'*) the initial composition and compositions containing (*2*, *2'*) polyetherimide and (*3*, *3'*) PSF which were cured at (a) 200 and (b) 180°C for 12 h and (c) 160–180–200°C for 2–4–2 h. The temperature scale corresponding to the scale of the time of heating of samples *t* is given to estimate their thermal stability.

Table 2. Kinetic parameters for the degradation of compositions based on the epoxy resin ED-20 and DADPS. Calculations were performed according to the Freeman-Carroll model

Cure mode		Kinetic parameters of the thermo-oxidative degradation of initial and modified compositions							
		$(\Delta\ln V)/(\Delta\ln W) = n + E[-\Delta(1/T)/R(\Delta\ln W)]$				$(\Delta\ln V)/\Delta(1/T) = n(\Delta\ln W)/\Delta(1/T) - (E/R)$			
T, °C	Time, h	α_{1-3}, %	ΔT, °C	n	E_{a1-3}, kJ/mol	α_{1-3}, %	ΔT, °C	n	E_{a1-3}, kJ/mol
ED-20 + DADPS									
160–180–200	2–4–2	0.4–9.1	393–409	>5	915 ± 50	1.0–10.0	385–401	>5	810 ± 50
		10.0–24.9	413–425	1.0	333 ± 30	10.4–21.1	401–419	1.0	360 ± 30
		24.9–67.8	425–441	0.5	227 ± 10	21.1–67.8	420–441	0.7	280 ± 10
180	12	4.0–8.6	363–369	>5	588 ± 50	1.9–7.1	372–388	>5	1000 ± 50
		9.0–37.0	372–404	0.5	286 ± 10	12.0–29.1	396–412	0.9	224 ± 10
		37.0–91.0	404–444	0.4	183 ± 10	42.3–78.1	420–436	0.32	149 ± 10
200	12	0.4–9.9	401–417	>5	857 ± 50	0.1–15.4	397–421	>5	914 ± 50
		9.9–22.0	417–425	1.0	375 ± 30	22.0–52.0	421–437	0.82	240 ± 10
		30.2–81.6	429–445	0.6	244 ± 10	52.0–99.0	437–449	0.30	110 ± 10
ED-20 + DADPS + polyetherimide									
160–180–200	2–4–2	2.3–10.3	352–368	>5	973 ± 50	0.3–5.0	352–368	>5	773 ± 50
		13.2–90.3	372–422	0.5	205 ± 10	9.0–73.0	376–416	1.3	199 ± 10
180	12	0.6–8.3	361–377	>5	775 ± 30	0.6–5.0	352–368	>5	582 ± 50
		11.5–83.6	381–433	1.0	170 ± 10	7.3–78.0	376–416	0.96	183 ± 10
200	12	1.5–20.7	400–412	>5	960 ± 50	0.4–4.6	402–410	>5	900 ± 50
		20.7–55.5	412–422	1.0	650 ± 50	4.6–20.0	406–420	1.4	540 ± 30
		55.5–94.1	422–436	0.5	250 ± 10	27.8–77.2	422–438	0.4	311 ± 10
ED-20 + DADPS + PSF									
160–180–200	2–4–2	0.6–9.0	291–304	1.0	530 ± 30	0.6–9.4	291–307	5.0	499 ± 30
		9.4–66.3	307–331	0.5	308 ± 10	9.4–66.3	307–331	0.5	199 ± 10
180	12	0.5–7.9	328–344	0.9	485 ± 30	0.5–7.9	328–344	5.2	485 ± 30
		19.4–99.0	352–376	0.45	223 ± 10	19.4–99.0	352–376	0.5	216 ± 10
200	12	1.8–9.4	341–345	>5	1000 ± 50	1.8–9.4	341–349	>5	963 ± 50
		16.0–26.3	345–361	1.0	500 ± 30	9.4–26.3	349–357	2.25	498 ± 30
		26.6–5.0	365–373	0.2	262 ± 10	26.3–99.0	361–400	0.14	274 ± 10

180 and 200°C, respectively. In the incompatible system filled with polyetherimide, the onset temperature of degradation decreases by 40°C for the sample cured in the stepwise mode and increases slightly (by 5°C) for the sample cured at 200°C.

The ratio of activity parameters for the samples in the radical-chain oxidation process looks somewhat different. The values of the induction period change differently. For ED-20 + DADPS + polyetherimide samples cured at 180°C and in the stepwise mode, the induction period increases by 1.5 and 1.3 times, respectively, compared with ED-20 + DADPS samples. This circumstance suggests that propagation of the radical-chain process slows down. For the PSF-filled samples, τ_{ind} decreases by a factor of 1.2 in the case of the samples cured in the dropwise mode at 180°C and by a factor of 1.6 times in the case of the sample cured at 200°C. Hence, for the sample filled with PSF, the oxidation process of the epoxy matrix accelerates. The slopes of the linear anamorphoses of kinetic curves, first, show a well-defined tendency toward a decrease in the rate of propagation of oxidative degradation for the system filled with polyetherimide and its increase for the system filled with PSF (Table 1). This result conforms to the data derived from the ratio of induction periods. Second, the presence of inflections on the linear anamorphoses of the initial composition and the composition filled with polyetherimide which were cured at 200°C suggests that the mechanism of radical reactions occurring during development of the oxidation process changes. It is important that, for the composition with PSF as

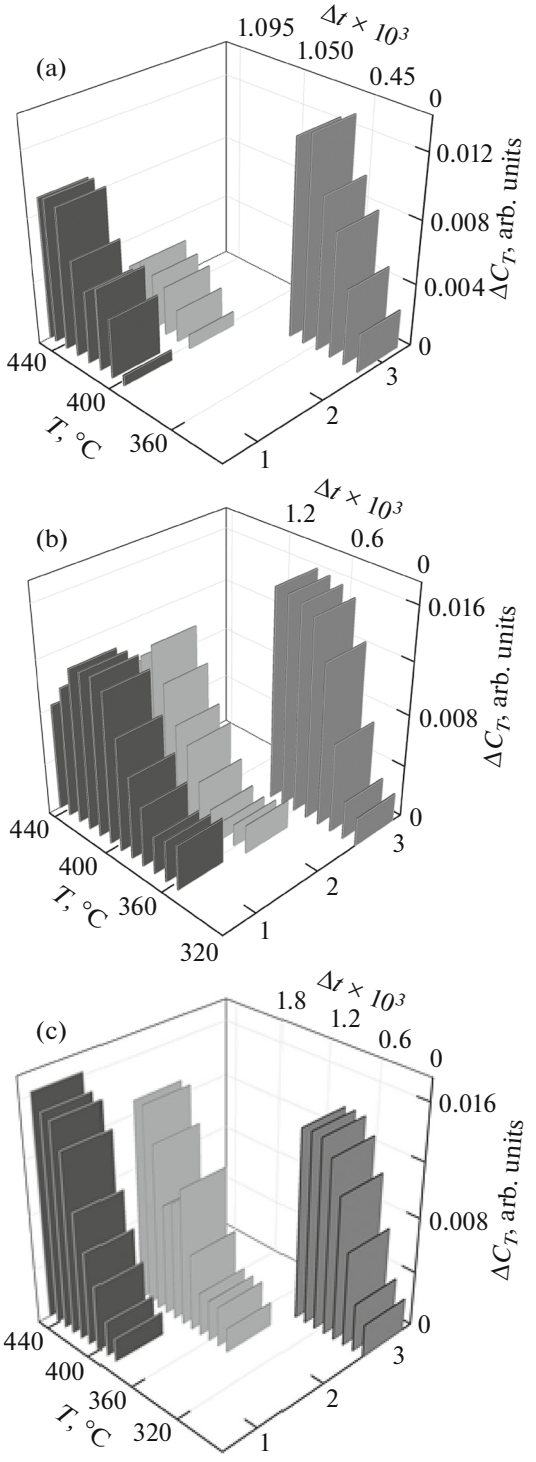

Fig. 3. 3D diagrams of the temperature–time dependence of change in the specific heat capacity ΔC_T during thermo-oxidative degradation of (*1*) epoxyamine compositions ED-20 + DADPS and the same compositions filled with (*2*) polyetherimide and (*3*) PSF which were cured at (a) 200 and (b) 180°C for 12 h and (c) 160–180–200°C for 2–4–2 h.

well as for the samples cured at 180°C and in the stepwise mode, there are no inflections and, hence, there is no such change in mechanism in the analogous temperature range. Possibly, the presence of inflections is related to the structure of the network preformed at 200°C. The process of oxidation and degradation of the samples with a looser network is more uniform.

Using the program Origin-8, the experimental data of the temperature–time dependences of a change in specific heat capacity which were obtained in the form of function $\Delta C_T = d(dH(t)/dt)/dT = f(t, T)$ at $dT = 8$°C for ED-20 + DADPS initial and filled epoxyamine compositions cured in different modes during thermo-oxidative degradation were interpolated in the 3D space. Figure 3 shows the resulting 3D diagrams for the compositions of different formulation. These diagrams graphically reflect a change in the rate of thermo-oxidative degradation (W_{O_2}) of active bonds during the process in proportion to their concentration in each temperature-time interval:

$$W_{O_2} = k_{2n}/(k_{6n})^{0.5}[R_nH][R_nO_2^{\bullet}]$$

$$dW_{O_2}/dt = d(dH(t)/dt)/dT.$$

We assume that a change in the heat capacity ΔC_T corresponds to a change in the concentration of active bonds participating in the degradation process in each structural element in the corresponding temperature–time interval and reflects the rate of the process. In this case, a comparison of ΔC_T values in temperature–time regions for different samples (Fig. 3) allows one to examine the distribution of active centers and weak bonds involved in the thermo-oxidative degradation of each sample and to trace the dynamics of their changes, that is, to reveal differences in the mechanism of the process.

It is also assumed that comparing the shape of intensity of the total figure reflecting the dependence $\Delta C_T = f(t, T)$ and the temperature–time regions of each element within it will make it possible to estimate the contributions of the rate of filler oxidation, the rate of breakage of bonds of the network preformed in the epoxy matrix, and the time of entry of each structural element into the oxidation process.

From an analysis of the figures of dependences $\Delta C_T = f(t, T)$, we can infer the following.

First, for the ED-20 + DADPS sample modified with PSF soluble in the epoxy oligomer, the entire figure considerably shifts to the low-temperature region. The shape of this figure indicates a monotonic gain in the concentration of active centers participating in the degradation reaction. As is seen from Figs. 3a and 3b, the cure of this sample at 180 and 200°C may cause an increase in the ultimate rate of degradation. For the sample cured in the stepwise mode (Fig. 3c), the ultimate rate of degradation decreases at the lowest onset temperature of the degradation process. These data suggest that the oxidation ability of the ED-20 +

DADPS + PSF samples grows most likely owing to oxidation of the filler. PSF initiates the thermo-oxidative degradation of the epoxy binder, and the process occurs under conditions close to homogeneous. The density of the network preformed in the epoxy matrix determines the mechanism of breakdown of the epoxy constituent.

Second, the initial temperature region of the figure for the sample ED-20 + DADPS + polyetherimide (thermoplastic incompatible with oligoether) is close to that for the initial epoxyamine composition, except the sample cured in the stepwise mode. This finding presumably suggests that the rate of oxidation of the modifier and the epoxy constituent are similar. An inspection of the figures of the dependence $\Delta C_T = f(t, T)$ for polyetherimide-containing samples shows that individual temperature–time elements corresponding to changes in the rate of thermo-oxidative degradation at deep stages of the process can be distinguished. This fact is evidence for its heterogeneous nature (Figs. 3a, 3b).

Third, a comparison of the figures for samples containing polyetherimide and PSF with that of the initial composition demonstrates a more pronounced effect of the network structure on degradation for the sample with the heterogeneous structure.

Fourth, a noticeable reduction in the intensity of the entire figure indicating a change in the rate of breakage of active bonds is observed for the sample cured at 200°C (12 h). For the composition cured in the stepwise mode, the onset of degradation considerably shifts to the low-temperature region and heterogeneity in elements of the figure becomes more distinct. This can be explained by a marked effect of heterogeneity of the network structure of the epoxy matrix on the manifestation of differences in the nature of breaking bonds of the epoxy polymer.

Thus, the effect of the modifier on the kinetics and mechanism of the process may be explained by the compatibility of the modifier with the epoxy oligomer. Compatible modifiers activate the process of breakage of polymer bonds in the homogeneous process. For the sample modified with incompatible polyetherimide, the degradation process is of a heterogeneous nature.

To Determining Mechanisms of Reactions Occurring in Modified Epoxy Compositions under Heating at One Constant Rate

To reveal mechanisms of thermo-oxidative degradation in the tested compositions, the activation energy, pre-exponential factor, and reaction order were calculated. To this end, we used kinetic models [29–37] relying on the temperature dependence of the rate of the process V, the value of conversion in the form of relation $W = 1-\alpha$, and the rate of change in polymer conversion dW/dt during heating of the sample at a constant rate β. This approach to solving the problem was previously used in [20, 31].

In accordance with the concepts of thermal kinetics, the rate of change in conversion per unit time t is

$$V = dW/dt = k(T)f(\alpha); \quad (2)$$

i.e., expression (2) includes the temperature dependence of two parameters, the reaction rate constant and the conversion constituent. The temperature dependence of the reaction rate constant $k(T)$ obeys the Arrhenius equation:

$$k(T) = A\exp(-E_a/RT),$$

where T is the absolute temperature (K) and R is the universal gas constant.

The conversion constituent $f(\alpha)$ may be represented by the expression

$$f(\alpha) = (1-\alpha)^n = W^n.$$

Taking into account the temperature dependences of $k(T)$ and $f(\alpha)$, Eq. (2) may be written as follows:

$$V = dW/dt = AW^n\exp(-E_a/RT) \quad (3)$$

or in the logarithmic form:

$$\ln V = \ln(-dW/dt) = \ln A + n\ln W - E/RT. \quad (4)$$

Usually for the nonisothermal regime at a constant heating rate (β = const), Eq. (3) is applied in the differential or integral form. In this work, we used Freeman–Carroll models [30] based on the differential form of Eq. (4):

$$\Delta\ln V = \Delta\ln(-dW/dt) = n\Delta\ln W - (E_a/R)\Delta(1/T). \quad (5)$$

The values of the activation energy and the reaction order were calculated using two modifications of Eq. (5) in the form

$$(\Delta\ln V)/(\Delta 1/T) = n[D\ln W/\Delta(1/T)] - (E/R), \quad (6)$$

$$(\Delta\ln V)/(\Delta\ln W) = n + E[-\Delta(1/T)/R\,(\Delta\ln W)]. \quad (7)$$

The values of n and E_a were obtained from plots obtained in coordinates

$$(\Delta\ln V)/(\Delta 1/T) = f[\Delta\ln W/\Delta(1/T)], \quad (8)$$

$$[(\Delta\ln V)/(\Delta\ln W)] = f[-\Delta(1/T)/R\,(\Delta\ln W)], \quad (9)$$

where the slope of the rectilinear dependence (8) corresponds to the reaction order n and the intercept at $[\Delta\ln W/\Delta(1/T)] = 0$ yields the value of $-E/R$; in expression (9), the values of the slope and intercept are E_a and n, respectively.

Dependences (8) and (9) were obtained for all the tested samples. Figure 4 shows the examples of kinetic curves for the epoxyamine compositions ED-20 + DADPS cured at 200 and 180°C and in the stepwise mode (curves *1–3*, respectively). Table 2 lists the kinetic parameters derived from the specified dependences.

Our experimental data show that, first, the plots of these dependences are linear anamorphoses consist-

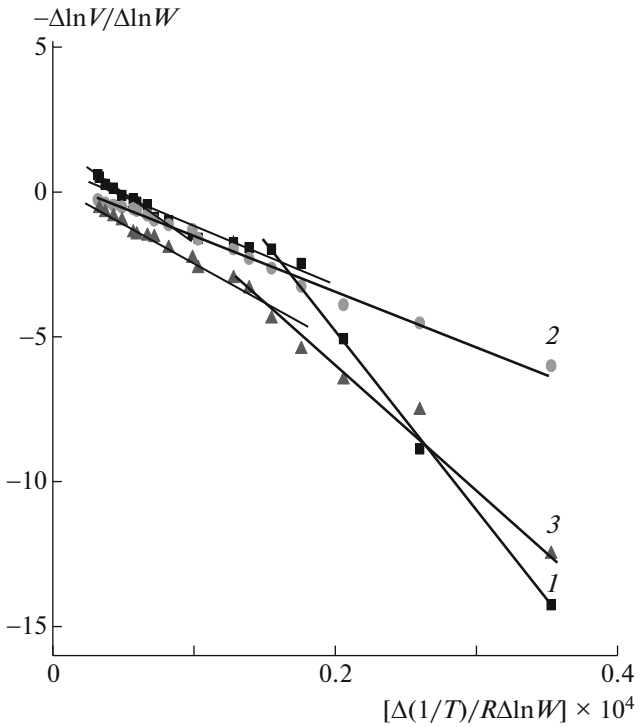

Fig. 4. Kinetic curves of the temperature dependence describing thermo-oxidative degradation in terms of the Freeman–Carroll model in coordinates $[(\Delta \ln V)/(\Delta \ln W)] = f[-\Delta(1/T)/R(\Delta \ln W)]$ for ED-20 + DADPS samples precured at (*1*) 200 and (*2*) 180°C for 12 h and (*3*) 160–180–200°C for 2–4–2 h.

ing of several regions that differ in position on the temperature scale and slope, that is, have different E_a values (Fig. 4). As follows from the intercepts of these regions, along with differences in activation energies, these temperature regions correspond to different values of the reaction order n; hence, they may be attributed to different stages of thermo-oxidative degradation having different kinetic parameters. Second, as is clear from Table 2, the values of the kinetic parameters describing processes occurring at initial (up to $\alpha \sim 10–15\%$) and deeper stages of thermal oxidation are different. For all the studied compositions, the initial stage of degradation is characterized by abnormally high values of the activation energy (from 600 to 1000 kJ/mol) and the reaction order ($n \gg 5$). At a higher conversion of the sample, the values of the activation energy and the reaction order decrease substantially in the high-temperature region. On the kinetic curve, one can distinguish not one but two regions with different E_a values depending on the nature and structure of the samples. For example, for all the tested compositions cured at 200°C and unfilled samples cured at 180°C and in the stepwise mode, each high-temperature region has two values of E_a and n (Table 2). Modified samples cured at 180°C and in the stepwise mode are characterized by the same values of high-temperature E_a and n.

To more accurately determine the kinetic parameters of thermo-oxidative degradation Friedman and Ozawa models were used [30–36]. In accordance with the Friedman–Ozawa model, to derive the kinetic parameters, Eq. (4) was transformed as applied to the constant heating rate for the pseudo-first order reaction using the plot of the linear dependence of the rate of polymer conversion on temperature in coordinates

$$\ln[(-dW/dt)/W] = f(-1/RT), \qquad (10)$$

where the slope of the line is E_a.

As opposed to the differential models of process kinetics, the Coats–Redfern model uses the integral equation

$$\log[-\ln W/T^2] = \log(AR/\beta E)\,[1 - (2RT/E)] - E/2.303RT$$

In this work, the values of E_a were calculated from the slopes of straight lines on the figures of dependences plotted in coordinates

$$\log[-\ln(W/T^2)] = f(1/RT). \qquad (11)$$

The dependences were obtained using the Friedman–Ozawa and Coats–Redfern models. The examples of the latter for the unfilled samples and polyetherimide- and PSF-filled samples cured at 200°C are given in Fig. 5. It is seen that the experimental data also fall on the straight line with inflections corresponding to a low-temperature region with a high value of E_a and a high-temperature region with a low value of E_a on the temperature scale in much the same way as dependences (8)–(9) plotted according to the Freeman–Carroll model.

Table 3 lists the kinetic parameters characterizing the thermo-oxidative degradation of the samples which were calculated using these models. A comparison of the data demonstrates that there is satisfactory agreement between the values of kinetic parameters obtained for the same samples. Differences between the kinetic parameters of processes occurring at initial and deeper stages of thermo-oxidative degradation for all the tested samples of epoxyamine polymers confirm that this process is composed of several different stages.

An examination of the obtained parameters shows that the values of E_a estimated for each stage are high; this suggests the effectiveness of this parameter $E_{a.eff}$. These stages include several processes or different reactions. The value of $E_{a.eff}$ is the superposition of the values of E_a for these reactions. It is believed that the abnormally high kinetic parameters of degradation, including the activation energy of the process occurring to a polymer conversion of $\alpha \sim 10–15\%$ (600–1000 kJ/mol), the reaction order ($n \gg 5$), and the preexponent (Table 4), are associated with the superposi-

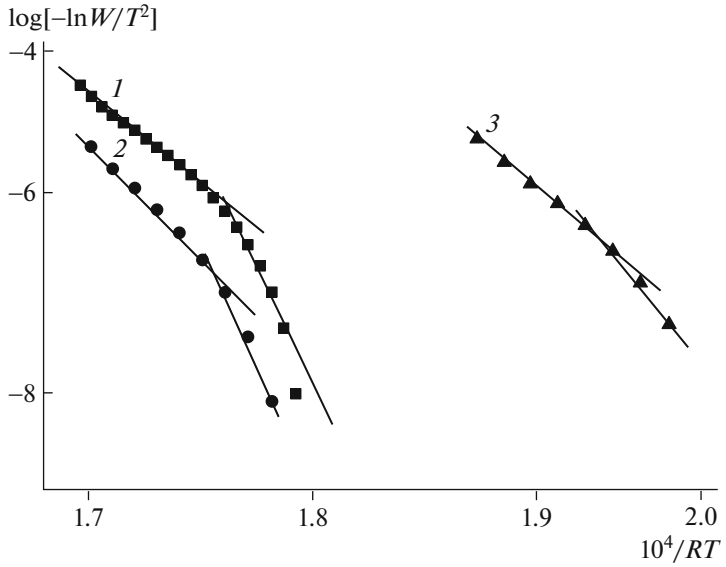

Fig. 5. Kinetic curves of the temperature dependence describing the process of thermo-oxidative degradation in terms of the Coats–Redfern model in coordinates log [–lnW/T^2] = $f(1/RT)$ for (*1*) ED-20 + DADPS, (*2*) ED-20 + DADPS + polyetherimide, and (*3*) ED-20 + DADPS + PSF samples cured at 200°C for 12 h.

tion of diffusion processes and chemical reactions. In this case, diffusion processes limit this stage of the process. A marked reduction in the values of $E_{a.eff}$ (to 400–200 kJ/mol or below), A, and n (to 1.0–0.2) after inflection on the kinetic curves at a conversion of ~20% implies that, at this stage of thermal oxidation, the effective values of the parameters are associated with the occurrence of chemical reactions. Diffusion processes may be caused by the relaxation processes of unfreezing of the segmental mobility of macrochains in network junctions, movement of active species involved in chemical reactions, and inhibition of oxygen supply to the reaction zone by filler particles and/or molecules.

The highest values of $E_{a.eff}$ and n for the samples cured at 200°C (Table 2) may be explained by a high density of the network in which macrochain units have a low segmental mobility [3, 7, 8, 17, 20, 37]. There is a tendency to a certain rise in the initial values of the activation energy for ED-20 + DADPS samples filled with polyetherimide and PSF. For the samples with a looser network formed at 180°C and in the stepwise cure mode, the values of $E_{a.eff}$ are much smaller than those for the samples cured at 200°C (Table 2). For the samples containing PSF, the value of E_a is lower than that for the initial composition ED-20 + DADPS and the composition containing polyetherimide (Table 3). In the case of the system ED-20 + DADPS + polyetherimide, the initial values of the activation energy are 775 and 973 kJ/mol for the samples cured at 180°C and in the stepwise mode, respectively. For ED-20 + DADPS samples cured at 180°C and in the stepwise mode, E_a is 588 and 915 kJ/mol, respectively. For the samples filled with PSF and cured at 180°C and in the stepwise mode, E_a is 485 and 530 kJ/mol, respectively.

The higher effective kinetic parameters for the samples precured at 200°C which correspond to the inhibition of thermo-oxidative degradation at the initial stage, for example, during the induction period, are related to a lower activity of these samples, a smaller change in the specific heat capacity ΔC_T, and a higher initial temperature. Reduction in these effects for the samples with a lower density of the network indicates that structural parameters play a considerable role just at the initial stage of thermal oxidation of epoxyamine compositions.

As follows from the data obtained for the samples with different compatibility of components and cured in different modes (Table 3), considerable differences in polymer conversions and reaction orders are observed in the high-temperature region after conversion $\alpha > 15$–20%. The existence of several inflections on the kinetic curves can apparently be explained by the superposition of reactions simultaneously occurring in the polymer according to different mechanisms.

At the first stage corresponding to the polymer conversion above 20%, the values of the activation energy approach 250–300 kJ/mol, as is typical of the breakage of C–C bonds [38], and the reaction order tends to 1.0 or 0.6–0.7. In the second high-temperature interval, the value of n is within 0.5–0.3 and E_a takes a much lower value (82–90 kJ/mol and matches the radical-chain thermo-oxidative degradation process [38]). For the polyetherimide- and PSF-containing samples cured under conditions when the loose

Table 3. Effective activation energies of thermo-oxidative degradation processes in epoxy compositions filled with polyetherimide and PSF calculated using various kinetic models

Cure mode		Freeman–Carroll equation $(\Delta\ln V)/(\Delta\ln W) = n + E[-\Delta(1/T)/R(\Delta\ln W)]$				Friedman equation $[-(dW/dt)/W] = f(-1/RT)$				Coats–Redfern equation $\log[-\ln W/T^2] = f(1/RT)$		
T, °C	Time, h	ΔT, °C	$\Delta\alpha$, %	E_a, kJ/mol	n	ΔT, °C	$\Delta\alpha$, %	E_a, kJ/mol	A, s^{-1}	ΔT, °C	$\Delta\alpha$, %	E_a, kJ/mol
ED-20 + DADPS												
160–180–200	2–4–2	393–417	0.4–12.0	540 ± 50	>5	393–420	0.4–12.0	500 ± 50	2×10^{34}	393–420	0.4–12.0	336 ± 50
		420–444	12–68	280±10	1.0	420–444	12–78	330 ± 10	1×10^{24}	420–444	12–68	282 ± 10
180	12	396–420	1.2–12.0	588 ± 50	>5	396–420	1.2–12.0	387 ± 50	1.5×10^{25}	396–420	1.2–12.0	430 ± 50
		420–436	12–78	290 ± 10	0.7	420–436	12–78	253 ± 10	1.6×10^{15}	420–436	12–78	202 ± 10
200	12	397–420	1–12	857 ± 50	>5	397–421	1–12	755 ± 50	2×10^{54}	397–420	1–12	809 ± 50
		420–436	12–78	275 ± 10	0.7	420–436	12–78	370 ± 10	2×10^{24}	420–436	12–78	423 ± 10
ED-20 + DADPS + polyetherimide												
160–180–200	2–4–2	352–376	0.4–8.0	773 ± 50	>5	352–376	0.4–8.0	360 ± 50	8.4×10^{26}	352–376	0.4–8.0	282 ± 50
		376–416	8–73	212 ± 10	1.0	376–416	8–73	270 ± 10	1.7×10^{18}	376–416	8–73	110 ± 10
180	12	352–376	0.6–4.0	810 ± 50	>5	352–376	0.6–4.0	385 ± 50	4.6×10^{28}	352–376	0.6–4.0	492 ± 50
		376–433	4–77	162 ± 10	1.0	376–433	4–77	230 ± 10	1.6×10^{15}	376–433	4–77	262 ± 10
200	12	412–426	5–41	512 ± 50	1	412–426	5–41	510 ± 50	1.2×10^{39}	412–426	5–41	540 ± 50
		426–440	41–77	210 ± 10	0.75	426–440	41–77	260 ± 10	6.4×10^{17}	426–440	41–77	260 ± 10
ED-20 + DADPS + PSF												
160–180–200	2–4–2	291–307	0.6–9.0	612 ± 50	>5	291–307	0.6–9.0	402 ± 50	1×10^{33}	291–307	0.6–9.0	280 ± 50
		307–331	9–66	280 ± 10	1	307–331	9–66	297 ± 10	3.8×10^{22}	307–331	9–66	187 ± 10
180	12	328–340	0.5–8.0	500 ± 50	5	328–340	0.5–8.0	493 ± 50	7.5×10^{33}	328–340	0.5–8.0	390 ± 50
		340–370	8–68	315 ± 10	0.5	340–368	8–68	340 ± 10	1.4×10^{22}	340–368	8–68	173 ± 10
200	12	341–357	2–9	500 ± 50	2.8	341–357	1–9	730 ± 50	4.3×10^{58}	–	–	–
		357–370	9–76	260 ± 10	0.2	357–370	9–76	430 ± 10	2.3×10^{33}	350–369	9–76	437 ± 50

network is formed, the role of the inhibiting or initiating ability of the filler may be identified at high conversions of the polymer.

For a more detailed study of filled epoxyamine composites, it was assumed that the overall process of thermo-oxidative degradation is composed of several independent exothermic reactions. Since the distribution of temperature within the sample is uniform and the time of heat loss is linear with temperature in different fractions of the polymer substance, that is, in reactants 1, 2, 3, ..., j, then using Moukhina models [39, 40] the process may be depicted by the following scheme:

$$d[RH_1]/dt = f_1(\theta_1, C_1, t_1)$$
$$d[RH_2]/dt = f_2(\theta_2, C_2, t_2)$$
$$d[RH_3]/dt = f_3(\theta_3, C_3, t_3)$$
$$d[RH_4]/dt = f_4(\theta_4, C_4, t_4),$$

where for the DADPS-cured ED-20 composition with polyetherimide or PSF fillers [RH] is the total concentration of reactive active centers involved in the degradation process; $[RH_1]$–$[RH_4]$ are the concentration of terminal groups of the epoxy polymer, units in network junctions, units in interjunction chains, and reactive groups in modifiers, respectively; θ_{1-4} are the kinetic parameters of bond breakage reactions; and t is the time of degradation.

The composition of the filled epoxy polymer is a heterogeneous system, and its kinetic equations include the activation energy and pre-exponent parameters which are not constant values [41]. In the systems, there exists the exchange of free valence between various active centers and there is the intermolecular transfer of kinetic chains of oxidation and degradation. The macromolecular nature and specific features of the network structure create restrictions for the redistribution of energy between active centers and

Table 4. Kinetic parameters of the thermo-oxidative degradation of fractions of the cured initial composition ED + DADPS and the same composition filled with polyetherimide and PSF

Stage of thermo-oxidative degradation	Cure mode		Parameters of thermo-oxidative degradation			
	T, °C	time, h	ΔT, °C	α, %	E_a, kJ/mol	A, s^{-1}
ED-20 + DADPS						
I	160–180–200	2–4–2	356–380	0.5–4.0	430	10^{31}
	180	12	401–410	5–29	330	10^{23}
	200	12	412–424	7–22	361	10^{31}
II	160–180–200	2–4–2	380–412	4.0–29.2	250	10^{17}
	180	12	410–430	30–50	270	10^{13}
	200	12	425–449	22–62	254	10^{19}
III	160–180–200	2–4–2	412–444	29.1–78.0	157	10^{11}
	180	12	429–438	52–72	165	10^{10}
	200	12	449–459	62–97	176	10^{12}
IV	160–180–200	2–4–2	449–459	80–97	94	10^{5}
	180	12	438–450	72–90	96	10^{5}
	200	12	–	–	–	–
ED-20 + DADPS + polyetherimide						
I	160–180–200	2–4–2	360–368	1.8–4.5	360	10^{26}
	180	12	360–368	1.5–4.5	300	10^{29}
	200	12	412–420	7.0–22.0	361	10^{29}
II	160–180–200	2–4–2	368–384	4.5–14.5	244.5	10^{17}
	180	12	368–377	4.5–14.5	180.5	10^{15}
	200	12	420–428	22.0-49.0	292.0	10^{19}
III	160–180–200	2–4–2	384–400	14.5–37.0	222	10^{15}
	180	12	377–388	14.5–37.0	100	10^{8}
	200	12	428–438	50.0–97.5	213	10^{15}
IV	160–180–200	2–4–2	400–424	37.0–97.0	166	10^{10}
	180	12	388–428	58–80	70	10^{5}
	200	12	–	–	–	–
ED-20 + DADPS + PSF						
I	160–180–200	2–4–2	380–400	3.0–13.3	273	10^{19}
	180	12	380–400	3.0–16.0	341	10^{27}
	200	12	406–418	10.0–35.2	423	10^{30}
II	160–180–200	2–4–2	400–420	13.0–42.0	180	10^{15}
	180	12	400–420	13.3–42.5	218	10^{15}
	200	12	412–426	35.0–56.0	231	10^{17}
III	160–180–200	2–4–2	420–440	42.5–88.0	157	10^{10}
	180	12	418–426	42.5–88.0	160	10^{13}
	200	12	420–440	56.0–88.0	178.5	10^{12}
IV	160–180–200	2–4–2	438–448	88.0–97.0	62.5	10^{4}
	180	12	438–448	88.0–97.0	62.5	10^{4}
	200	12	438–448	85.0–97.0	70.0	10^{5}

reactive functional groups. As a result, the distribution of reactive centers over kinetic parameters appears. For such systems, the kinetic curve $C(t)$ is determined as an integral:

$$[\mathrm{RH}](t) = \int_0^k G(k,t)f(k)dk,$$

where $f(k)$ is the function of distribution over rate constants and $G(k, t)$ is the system of ordinary differential equations of the first order modeling the kinetics for individual kinetic ensembles.

To analyze the kinetic curves and to derive the distribution of kinetic parameters, we proposed a system of integral equations modeling the polychronic process:

$$[\mathrm{RH}_1](t) = \int_0^k G_1(k,t)f_1(k)dk,$$

.....

$$[\mathrm{RH}_j](t) = \int_0^k G_j(k_i,t)f_j(k_i)\Delta k_i$$

Instead of each of the integrals, we may write their sum:

$$[\mathrm{RH}_j](t) = \sum_0^k G_j(k,t)f_j(k)dk$$

in the differential form with respect to time

$$\frac{d[\mathrm{RH}_j]}{dt} = \sum_0^k \frac{dG_i(k_i,t)}{dt} f_j(k_i)\Delta k_i,$$

where $d[\mathrm{RH}_j]/dt$ is the rate of the jth reaction and $d\Delta H_i/dt$ is a part of the equation modeling degradation of the jth component of the epoxy composition.

In accordance with this model, the heat balance equation may be written as

$$\begin{aligned}[\mathrm{RH}_j]dT/dt &= [\mathrm{RH}_1]\Delta H_1 A_1 \exp(-E_1/RT) f(\alpha_1) \\ &+ [\mathrm{RH}_2]\Delta H_2 A_2 \exp(-E_2/RT) f(\alpha_2) + \ldots \\ &= [\mathrm{RH}_i]\Delta H_i A_i \exp(-E_i/RT) f(a_i) - \alpha s/V(T - T_0).\end{aligned}$$

The consumption of reactants $[\mathrm{RH}_1]$, $[\mathrm{RH}_2]$, ..., $[\mathrm{RH}_j]$ may be represented in the form of a relative value, the conversion of component α. The consumption of reactants may be described by the following equations:

$$-d\alpha_1/dt = A_1 \exp(-E_{a1}/RT) f(\alpha_1),$$

$$-d\alpha_2/dt = A_2 \exp(-E_{a2}/RT) f(\alpha_2),$$

.....

$$-d\alpha_j/dt = A_j \exp(-E_{aj}/RT) f(\alpha_j).$$

A change in the temperature of the medium may be written as

$$T_0 = T_j + \beta t.$$

The initial conditions are $T = T_0 = T_i$ and $\alpha_1 = \alpha_2 = \ldots = \alpha_i = 0$ at $t = 0$; ΔH_i is the thermal effect of the jth reaction; E_{aj} is the activation energy of the jth reactant; A_j is the Arrhenius pre-exponent for the jth reaction or the frequency factor; $\alpha_1\ \alpha_2\ \ldots\ \alpha_j$ is the conversion of fraction 1, 2, 3, ... of the jth reactant over time t; and αs is the heat transfer coefficient. The values of parameters with index j refer to reactions 1, 2, 3, ..., j.

On the kinetic curves of heat release obtained for each sample, individual regions (stages) were isolated. The task of determining the temperature interval introduced in the heat balance equation was solved by the Tikhonov method [42]. For the isolated regions, the dependences of the rate of change in conversion on time and temperature were obtained and the values of E_{aj} and frequency factor A_j were calculated. The calculation results are summarized in Table 4. The calculated values of α, E_{aj}, and A_j characterizing each component (fraction) of the epoxy composition which participates in reaction in accordance with its local structure describe the process of breakage of bonds with different activity with respect to oxygen and its mechanism and make the corresponding contribution to the overall process. Accordingly, the number of fractions and their parameters vary with the sample structure and filler nature. The number of fractions is consistent with a set of reactions that can occur in the sample. An analysis of the values of E_a and A characterizing each fraction makes it possible to state that the thermo-oxidative degradation of the tested compositions may include three or more sequential processes depending on the sample. The main contribution to the thermo-oxidative degradation of all samples is provided by the breakage of C–C bonds of the epoxy binder. For example, the degradation of the initial ED-20 + DADPS sample having the dense network (cured at 200°C) occurs via three stages, while the degradation of the samples having the loose network proceeds via four stages. The first fraction, which can include up to 30% broken chains, makes itself evident in the temperature range of 350–420°C with E_a = 330 ± 50 kJ/mol and $A \sim 10^{22-27}$. The second fraction, accounting for 30–50% polymer, has lower values of $E_a = 270 \pm 20$ kJ/mol and $A = 10^{17-18}$, and, finally, the third fraction (α = 50–80%) and the fourth fraction (α = 80–97%) correspond to E_a = 175 ± 20 at $A = 10^{11-12}$ and 85 ± 15 kJ/mol at $A = 10^{5-8}$. The values of oxidation parameters of the first fraction indicate that the process taking place at this stage may be attributed to polymer degradation initiated by macroradicals [38]. The accumulation of overstressed chains and the breakage of weak bonds resulting in the generation of macroradicals may occur in the induction period.

In the temperature range of 350–400°C, the reaction of isomerization of the epoxy group to the carbonyl one which is accompanied by the exothermic

effect may proceed; the value of E_a for this reaction is 214 kJ/mol [38]. The same stage of the process may be related to the breakage of active bonds in stacks between chains localized in the network and interchain bonds capable of breakage with an activation energy of 185–223 kJ/mol [38]. According to parameters of the fourth stage, this value is due to the radical chain process of the thermo-oxidative degradation of chains of the cured epoxy resin. This process has the activation energy in the range from ~92 to 120 kJ/mol [38]. It should be noted that, during thermal oxidation through intermediate radicals, the transfer of the kinetic chain either to the aliphatic bond in interjunction chains or via the reaction of intramolecular substitution in the aromatic ring occurs. The higher values of E_a and pre-exponent of different fractions can apparently be explained by a high density of the network and a low segmental mobility of interjunction chains. The values of these parameters show that processes with the participation of intermediate radicals can take place which ensure the transfer of kinetic oxidation chains to C–C bonds of the aromatic unit or interjunction aliphatic chains.

For the filled samples, the nature of a change in the kinetic parameters on passage from one fraction to another during thermo-oxidative degradation and intervals within which the values of E_a and A change are similar to those of unmodified epoxyamine polymers. This finding evidently indicates that the process of destruction of the epoxy matrix predominates. The observed changes in parameters E_a and A may be related to the rate of oxygen supply or free valence transfer by radicals of the epoxy matrix to active centers or functional bonds of fillers. The filler may also change the process parameters owing to the participation of radicals in inhibition of the chain process in the case of polyetherimide or its initiation in the case of PSF.

The density of the epoxy polymer may change as a result of localization of the filler between junctions of the formed network. Since cure of the epoxy binder in the presence of polyetherimide leads to the formation of labile physical bonds, the junctions of the formed network become protected from stress which may appear in it. This leads to the predominant breakage of bonds in interjunction bridges and the transition of the degradation process to the chain oxidation of aliphatic bonds. The localization of the polyetherimide filler between network junctions increases the density of the polymer and the diffusion coefficient increases; as a consequence, the negative activation energy for the second–fourth fractions of the polymer somewhat increases; i.e., the rate of the process decreases (Table 4).

In the sample containing PSF, the latter decomposes into radicals and initiates their generation in the epoxy matrix during the induction period of thermal oxidation and thus shortens it. Since the system is compatible, the kinetically controlled reactions of the breakage of C–C bonds rapidly transform into the chain oxidation process most likely of more mobile aliphatic regions of interjunction chains. The initiation of degradation can occur owing to the decomposition of hydroperoxides accumulated during the thermal oxidation of C–H bonds of aliphatic regions in interjunction bridges. Therefore, the negative activation energy decreases sharply, which indicates an increase in the rate of the process.

During thermal oxidation through intermediate radicals, the transfer of kinetic chains appears either to the aliphatic bond in interjunction chains or via the reaction of intramolecular substitution in the aromatic nucleus. The transfer of kinetic chains is accompanied by the appearance of weak bonds accelerating the breakdown of chains [38]. To gain more detailed insight into the effect of fillers on the mechanism of thermal oxidation of the epoxyamine polymer, it is necessary to ascertain reactions which can take place in the tested samples of epoxyamine compositions with polyetherimide and PSF filers. With this aim in view, the composition of nonvolatile products of their oxidation was studied.

Nonvolatile Oxidation Products

IR spectroscopy was used to study the composition of nonvolatile products accumulating in the composition film samples during thermal oxidation under isothermal conditions. Epoxy-, carbonyl-, and hydroxyl-containing compounds were chosen as the main products. The composition of these products was assessed from the intensities of bands at 915, 1725, and 3450 cm^{-1} corresponding to the vibrations of epoxy, >C=O, and OH groups, respectively. For each sample, the change in the content of individual groups and in the ratios between them was estimated as a function of the time of oxidation. An analysis of the obtained data showed that there are differences in the composition of the products at the quantitative level and in the kinetics of change in their content during the process (Table 5). It is seen that the composition of the products is affected by the filler nature and network structure. There is a sharp difference between the samples with dense and loose networks. For example, in oxidation of the initial epoxyamine composition with the dense network (cured at 200°C for 12 h), the concentrations of OH and epoxy groups monotonically decrease and after 24 h drop by ~2 and 3 times, respectively, while the concentration of >C=O groups increases by 4.4 times during oxidation for the first 12 h and remains unchanged at a deeper oxidation. For the loose sample cured at 180°C, the content of OH and epoxy groups decreases by a factor of 1.4 over 24 h and the content of carboxyl-containing groups grows by a factor of 17.5 for the first 12 h and then remains invariable. For the sample cured in the stepwise mode, the content of OH groups decreases by a factor of

Table 5. Content of oxidation products at 180°C for compositions based on ED-20 and DADPS with polyetherimide and PSF fillers (IR data)

Cure mode		Oxidation time, h	Nonvolatile degradation products			Ratios between contents of functional groups			
T, °C	time, h		D_{3450}/D_{1840} (–OH)	D_{1725}/D_{1840} (>C=O)	D_{915}/D_{1840} (epoxide)	$D_{>C=O}/D_{OH-}$	$D_{>C=O}/D_{epoxy}$	$D_{epoxy}/D^0_{epoxide}$	$D_{>C=O}/D^0_{>C=O}$
ED-20 + DADPS									
160–180–200	2–4–2	0	8.1	2	1.1	0.25	0.14	1.0	1.0
		12	6.7	3.6	1.0	0.54	0.15	0.90	1.80
		24	6.7	7.9	0.7	1.18	0.10	0.64	3.95
180	12	0	9.8	0.4	1.4	0.041	0.14	1.0	1.0
		12	9.0	7.0	1.1	0.78	0.12	0.80	17.5
		24	7.0	7.0	1.0	1.0	0.14	0.70	17.5
200 (oxidation at 200°C)	12	0	11.0	2.6	2.2	0.24	0.20	1.0	1.0
		12	7.9	11.5	1.0	1.45	0.13	0.45	4.42
		24	5.3	11.5	0.7	2.17	0.13	0.32	4.42
ED-20 + DADPS + polyetherimide									
160–180–200	2–4–2	0	9.0	3.7	1.5	0.41	0.17	1.0	1.0
		12	7.5	4.4	1.4	0.59	0.19	0.93	1.20
		24	5.5	6.0	1.3	1.09	0.24	0.87	1.62
180	2–4–2	0	5.4	3.2	0.6	0.59	0.11	1.0	1.0
		12	3.5	4.2	0.5	1.20	0.14	0.83	1.30
		24	2.8	6.6	0.4	2.36	0.14	0.67	2.10
200 (oxidation at 200°C)	2–4–2	0	5.5	4.3	1.1	0.78	0.20	1.0	1.0
		12	4.6	4.7	1.0	1.02	0.22	0.90	1.09
		24		4.8	0.8	1.12	0.19	0.73	1.12
ED-20 + DADPS + PSF									
160–180–200	2–4–2	0	11.5	1.0	2.3	0.09	0.20	1.0	1.0
		12	9.0	2.5	1.4	0.28	0.16	0.61	2.50
		24	3.7	5.3	1.0	1.43	0.27	0.43	5.30
180	2–4–2	0	7.8	2.0	1.6	0.26	0.21	1.0	1.0
		12	5.5	3.0	1.0	0.55	0.18	0.62	1.50
		24	4.6	3.8	0.5	0.83	0.11	0.31	1.90
200 (oxidation at 200°C)	2–4–2	0	2.7	1.2	1.4	0.44	0.52	1.0	1.0
		12	2.5	2.0	1.3	0.80	0.52	0.93	1.67
		24	2.5	2.8	0.6	1.12	0.24	0.43	2.30

D^0 denotes the initial content of functional groups.

1.2 for the first 12 h and the content of epoxy groups monotonically decreases by a factor of ~1.6 for 24 h. In this case, the content of >C=O groups monotonically increases by a factor of 4.

The introduction of modifiers affects the mechanism of the process. The composition of the products changes more slowly during oxidation. Oxidation of the ED-20 + DADPS + polyetherimide sample having the dense network (cured at 200°C) for 24 h leads to a decrease in the content of OH and epoxy groups by ~1.3 times and in the content of >C=O groups by 1.1 times. For the samples with the loose structure cured at 180°C and in the stepwise mode upon oxidation for 24 h, the content of OH groups decreases by

1.6–1.9 times and the content of epoxy groups decreases by 1.1–1.5 times, while the content of >C=O groups increases by 1.6–2.0 times.

For the ED-20 + DADPS + PSF sample with the dense network structure after oxidation for 24 h, the content of hydroxyl groups remains almost unchanged and the content of epoxy groups decreases, while the content of >C=O groups increases by 2.3 times (Table 5). For the samples with the loose network, the change in the composition of the products is more distinct. After oxidation for 24 h for the samples cured at 180°C and in the stepwise mode, respectively, the content of OH groups decreases by 1.7 and 3.1 times, the content of epoxy groups decreases by 3.2 and 2.3 times, and the content of carbonyl groups grows by 1.9 and 5.3 times.

From the above data we can draw the following conclusions.

First, for all the epoxyamine samples with an increase in the degree of the process, the content of hydroxyl and epoxy groups decreases, while the content of carbonyl groups increases. The most pronounced change in the concentration of >C=O groups is observed for the sample with the loose network, while the most pronounced change in the concentration of epoxy and hydroxyl groups is detected for the sample with the dense network (Table 5).

Second, it is clear that the ratio between the concentrations of functional groups changes with the degree of the thermo-oxidative process, which may indicate that the mechanism of degradation reactions changes.

Using the ratios between various functional groups which were obtained for all the tested samples (Table 5), the main types of reactions able to proceed in the tested samples of the epoxy polymer during thermal oxidation in the isothermal regime were distinguished.

This is above all a decrease in the content of epoxy groups and an increase in the content of carbonyl groups related to the isomerization of epoxy groups to carboxyl ones.

The accumulation of OH and >C=O groups corresponds to the development of the radical chain process of thermal oxidation and thermo-oxidative degradation through hydroperoxide, as is typical of polyolefins. This process is apparently localized in interjunction units.

Finally, reduction in the concentration of epoxy and OH groups corresponds to the breakage of C–C bonds in the radical chain transfer of kinetic chains by radicals resulting from the decomposition of hydroperoxide.

According to a change in the ratio of various functional groups in the tested samples, it may be stated that the degree of cure considerably influences the mechanism of reactions. For incompletely cured samples, thermal oxidation and thermo-oxidative degradation prevail. This effect is observed in the case of the samples cured in the stepwise mode and at 180°C. For the samples with the dense network (cured at 200°C, 12 h) the thermo-oxidative degradation is slowed down and the processes of breakage of C–C bonds predominate.

The introduction of nanofillers in the epoxyamine composition changes the composition of functional groups, the rate of their accumulation, and the ratio between their concentrations in the oxidized samples. This finding indicates that the mechanism of the thermo-oxidative process changes.

As is clear from Table 5, the modification of ED-20 + DADPS changes differently the rate of consumption of OH groups and the rate of accumulation of >C=O groups. For the samples with the dense network which were cured at 200°C, the concentration of OH groups changes weakly for the sample with polyetherimide and remains almost the same for the sample with PSF. Given this, the rate of accumulation of >C=O groups for the sample containing PSF is higher compared with polyetherimide. Modification of the epoxyamine polymer increases the ratio between the content of >C=O and OH groups and decreases the rate of consumption of hydroxyl-containing groups.

For the samples with the dense network which were cured at 200°C and contain polyetherimide and PSF, the rate of consumption of OH groups and the rate of accumulation of >CO groups are lower compared with the unfilled sample.

For the samples with the loose network which were cured at 180°C, the ratios $[>C=O]/[>C=O]_0$ after oxidation for 24 h for the samples modified with PSF and polyetherimide increase by 1.90 and 2.06 times, respectively, against 17.5 times for the unmodified sample. At the same time, the ratios $[OH]/[OH]_0$ decrease by 1.9 and 1.7 times, respectively, against a ratio of 1.4 for the unmodified sample. According to these data, it can be inferred that modification of the epoxyamine polymer changes the mechanism of the process of transfer of kinetic chains during its thermal oxidation. A change in the ratio between the content of [>C=O] and [OH] groups during the thermo-oxidative degradation of modified samples may indicate that the process occurring by the radical chain mechanism predominates in which the intramolecular transfer of kinetic oxidation chains most likely proceeds within interjunction aliphatic bridges.

REFERENCES

1. L. Matějka, O. Dukh, and J. Kolařík, Polymer **41**, 1449 (2000).
2. S. Sun, P. Sun, and D. Liu, Eur. Polym. J. **41**, 913 (2005).
3. G. F. Novikov, E. V. Rabenok, L. M. Bogdanov, and V. I. Irzhak, Polym. Sci., Ser. A **59**, 741 (2017).

4. M. V. Saifutdinova, V. M. Mikhal'chuk, and R. I. Lyga, Vestn. Tverskogo Gos. Univ., Ser. Khim., No. 4, 188 (2016).

5. M. V. Saifutdinova, R. I. Lyga, V. M. Mikhal'chuk, and O. I. Dikhtenko, Vestn. Novgorod. Gos.Univ., No. 5 (103), 109 (2017).

6. Y. P. Gomza, V. V. Klepko, S. V. Zhil'tsova, V. M. Mikhal'chuk, L. A. Savenkova, T. E. Konstatinova, and V. A. Beloshenko, Polym. Sci., Ser. A **52**, 628 (2010).

7. S. O. Il'in, E. P. Plotnikova, M. L. Kerber, and I. Y. Gorbunova, Int. Polym. Sci. Technol. **39**, T57 (2012).

8. O. V. Akhmatova, S. V. Zyukin, Y. Kh. Vei, S. A. Smotrova, M. L. Kerber, V. S. Osipchik, and I. Yu. Gorbunova, Plast. Massy, No. 10, 55 (2010).

9. I. Y. Gorbunova, I. S. Sirotin, Y. V. Bilichenko, S. N. Filatov, M. L. Kerber, T. P. Kravchenko, and V. V. Kireev, Polym. Sci., Ser. B **57**, 402 (2015).

10. V. V. Kireev, I. D. Simonov-Emel'yanov, Yu. V. Bilichenko, K. A. Brigadnov, S. N. Filatov, N. V. Apeksimov, and A. R. Nikitina, Plast. Massy, Nos. 3–4, 26 (2016).

11. D. V. Onuchin, I. S. Sirotin, G. A. Pavlova, S. N. Filatov, V. V. Kireev, M. L. Kerber, I. Y. Gorbunova, Polym. Sci., Ser. B **60**, 182 (2018).

12. A. E. Chalykh, E. S. Zhavoronok, Z. A. Kochkova, and M. R. Kiselev, Russ. J. Phys. Chem. B **3**, 507 (2009).

13. R. I. Sopotov, S. V. Zyukin, V. A. Brodskii, M. L. Kerber, Yu. E. Doroshenko, and I. Yu. Gorbunova, Khim. Prom-st Segodnya, No. 11, 51 (2014).

14. M. P. Arinina, S. O. Il'in, V. V. Makarova, I. Y. Gorbunova, M. L. Kerber, and V. G. Kulichihin, Polym. Sci., Ser. A **57**, 177 (2015).

15. M. P. Arinina, V. A. Kostenko, I. Y. Gorbunova, S. O. Il'in, and A. Ya. Malkin, Polym. Sci., Ser. A **60**, 683 (2018).

16. D. Ch. Do, T. V. Khoang, V. S. Osipchik, S. A. Smotrova, and I. Yu. Gorbunova, Plast. Massy, No. 10, 53 (2010).

17. R. I. Sopotov, S. V. Zyukin, I. Yu. Gorbunova, M. L. Kerber, Yu. E. Doroshenko, T. P. Kravchenko, V. I. Il'in, and S. Yu. Tuzova, Plast. Massy, Nos. 11–12, 7 (2015).

18. *Polymer Composite Materials: Structure, Properties, Technology,* Ed. by A. A. Berlina (Professiya, Moscow, 2014) [in Russian].

19. E. V. Plakunova, E. A. Tatarintseva, and L. G. Panova, Plast.Massy, No. 1, 11 (2008).

20. L. S. Shibryaeva, I. Yu. Gorbunova, and M. L. Kerber, Russ. J. Phys. Chem. B **8**, 733 (2014).

21. C. Ciobany, D. Rosu, C. N. Cascaval, and L. Rosu, J. Macromol. Sci., Part A: Pure Appl. Chem. **38**, 991 (2001).

22. S. Terekhina, M. Mille, B. Fayolle, and X. Colin, Polym. Sci., Ser. A **55**, 614 (2013).

23. V. A. Kostenko, L. S. Bichevii, P. A. Povernov, N. V. Bornosuz, and I. Yu. Gorbunova, Usp. Khim. Khim. Tekhnol. **32** (6 (202)), 68 (2018).

24. R. I. Sopotov and I. Yu. Gorbunova, Usp. Khim. Khim. Tekhnol. **27** (3), 101 (2013).

25. L. S. Shibryaeva, *Progress in Physics and Chemistry of Polymers* (Khimiya, Moscow, 2004) [in Russian].

26. L. S. Shibryaeva, Yu. A. Reshmin, O. V. Shatalova, A. V. Krivandin, E. S. Kuksenko, I. Yu. Gorbunova, and M. L. Kerber, Polym. Sci., Ser. A **49**, 12 (2007).

27. Y. V. Tertyshnaya, L. S. Shibryaeva, and A. A. Ol'khov, Russ. J. Phys. Chem. B **9**, 498 (2015).

28. H.-J. Flammersheim and J. R. Opfermann, Macromol. Mater. Eng. **286**, 143 (2001).

29. J. D. Menczel and R. B. Prime, *Thermal Analysis of Polymers, Fundamentals and Applications* (Wiley, New York, 2009).

30. J. H. Chan and S. T. Balke, Polym. Degrad. Stab **57**, 135 (1997).

31. S. G. Kulichikhin, I. Yu. Gorbunova, M. L. Kerber, and E. V. Samardukov, Vysokomol. Soedin., Ser. B **37**, 533 (1995).

32. M. J. Starink, Thermochim. Acta **404**, 163 (2003).

33. T. J. Ozawa, J. Therm. Anal. **31**, 547 (1986).

34. T. J. Ozawa, Thermochim. Acta **355**, 35 (2000).

35. T. J. Ozawa, J. Therm. Anal. Calorim. **82**, 687 (2005).

36. P. Albu, C. Bolcu, G. Vlase, N. Doca, and T. Vlase, J. Therm. Anal. Calorim. **105**, 685 (2011).

37. T. F. Irzhak and V. I. Irzhak, Polym. Sci., Ser. A **59**, 791 (2017).

38. *Quick Reference Handbook on Physicochemical Quantities,* Ed. by K. P. Mishchenko and A. A. Ravdelya (Khimiya, Leningrad, 1974) [in Russian].

39. E. Moukhina, J. Therm. Anal. Calorim. **109**, 1203 (2012). https://doi.org/10.1007/s10973-012-2406-3

40. E. Moukhina, in *Proceedings of 39th North American Thermal Analysis Society Conference, Des Moines, Iowa, USA, 2011* (Des Moines, 2011), p. 335. https://doi.org/10.1177/0954008311409262

41. V. R. Pen, Khim. Rast. Syr'ya, No. 2, 101 (2004).

42. M. I. Sumin, *Regulation Methods of A. N. Tikhonova to Solve Operative equations of First Kind. Study Guide* (Nizhegorod. Gos. Univ., Nizhnii Novgorod, 2016) [in Russian].

Translated by T. Soboleva